

TOPICAL REVIEW

Water on surfaces from first-principles molecular dynamics^{*}

To cite this article: Peiwei You *et al* 2020 *Chinese Phys. B* **29** 116804

View the [article online](#) for updates and enhancements.

Water on surfaces from first-principles molecular dynamics*

Peiwei You(游佩桅)^{1,3}, Jiyu Xu(徐纪玉)^{1,3}, Cui Zhang(张萃)^{1,2,†}, and Sheng Meng(孟胜)^{1,2,3,4}

¹Beijing National Laboratory for Condensed Matter Physics and Institute of Physics, Chinese Academy of Sciences, Beijing 100190, China

²Songshan Lake Materials Laboratory, Dongguan 523808, China

³School of Physical Sciences, University of Chinese Academy of Sciences, Beijing 100049, China

⁴Collaborative Innovation Center of Quantum Matter, Beijing 100190, China

(Received 25 May 2020; revised manuscript received 25 May 2020; accepted manuscript online 3 July 2020)

Water is ubiquitous and so is its presence in the proximity of surfaces. To determine and control the properties of interfacial water molecules at nanoscale is essential for its successful applications in environmental and energy-related fields. It is very challenging to explore the atomic structure and electronic properties of water under various conditions, especially at the surfaces. Here we review recent progress and open challenges in describing physicochemical properties of water on surfaces for solar water splitting, water corrosion, and desalination using first-principles approaches, and highlight the key role of these methods in understanding the complex electronic and dynamic interplay between water and surfaces. We aim at showing the importance of unraveling fundamental mechanisms and providing physical insights into the behavior of water on surfaces, in order to pave the way to water-related material design.

Keywords: first-principles molecular dynamics, water at surfaces, reaction mechanism

PACS: 68.08.De, 73.22.-f

DOI: 10.1088/1674-1056/aba279

1. Introduction

The frontier basic research of water science has important applications in energy, environment, national defense, and other fields. The seemingly simple hydrogen oxygen composition of water presents extremely rich and complex structures and properties in different environments (surface, pressure, photoexcitation, etc.), which is a major challenge in the current scientific research.^[1–4] Determining and adjusting the electronic and dynamic properties of water in contact with surfaces at the atomic level are crucial to solve the essential problems in the wide applications of water.

One profound matter related to water at surfaces is hydrogen production, arising from photocatalytic water splitting, which provides a promising way to harvest solar energy and gain clean renewable energy.^[5–7] The most essential topic of photocatalytic water splitting is the interactions between water molecules and photocatalytic materials. A variety of photocatalytic materials have been discovered and intensely studied, such as metal oxides (e.g., TiO₂), sulfides (e.g., MoS₂), metal-free materials (e.g., g-C₃N₄), metal co-catalyst (e.g., Pt),^[6,8,9] and so forth. The most important aspects of semiconductor photocatalysts for water splitting are the size of band gap and the positions of conduction band minimum (CBM) and valence band maximum (VBM), which are critical to utilize most visible light from the solar spectrum and gain reasonable effi-

ciency of water splitting reaction. The microscopic insight into the fundamental properties and dynamic behaviors of the interplay between the liquid and photocatalysts may significantly improve the device performance and accelerate the process of material design. Research on the transport characteristics of water molecules and various ions/molecules in nanomaterials has also shown great application prospects in desalination, heavy metal pollution control, ion screening, and artificial biological channels.^[10–13]

First-principles approaches are effective means to unveil the microstructure and electronic properties of water at surfaces, providing both computational microscopes and predictive tools. The practical applications of first-principles methods based on density functional theory (DFT)^[14,15] rely on approximations for the exchange–correlation energy that describes the electron–electron interactions. The generalized gradient approximations (GGA)^[16] are the most popular forms for the exchange–correlation term, which provide reasonably accurate description of ground-state properties of solids, however, are inaccurate in describing the structure of liquid water at ambient conditions.^[17,18] Instead, hybrid exchange–correlation functionals can be employed to reduce the self-interaction error and alleviate the inaccuracies of GGA in describing liquid structure and electronic properties.^[19,20] Considering van der Waals (vdW) corrections

*Project supported by the National Key Basic Research Program of China (Grant Nos. 2016YFA0300902 and 2015CB921001), the National Natural Science Foundation of China (Grant Nos. 11974400, 91850120, and 11774396), and Strategic Priority Research Program B of the Chinese Academy of Sciences (Grant No. XDB070301).

†Corresponding author. E-mail: cuizhang@iphy.ac.cn

© 2020 Chinese Physical Society and IOP Publishing Ltd

<http://iopscience.iop.org/cpb> <http://cpb.iphy.ac.cn>

on the exchange–correlation interactions has been shown to improve certain properties of aqueous solutions, oxides, and 2D materials.^[21–23] Recently developed strongly constrained and appropriately normed (SCAN) functional is an important achievement of constructing non-empirical semi-local functional based on constraints. It can predict accurately the structure and energy information of various bonding systems, reaching the accuracy level of hybrid functionals, at the GGA level of computational cost.^[24,25] Semi-local functionals often fail in describing excited-state properties of water at surfaces quantitatively. The problem can be eased by the adoption of hybrid functionals and the DFT+ U approach, where U stands for the Hubbard correction,^[26,27] and the proper amount of exact exchange and the magnitude of the Hubbard correction are generally dependent on the system.

DFT combined with molecular dynamics gives birth to first-principles molecular dynamics (FPMD), providing a powerful tool to track dynamic change and evolution of interactions between the liquid and surfaces. Taking advantage of highly different dynamical characteristics of electrons and nuclei, the Born–Oppenheimer approximation, also known as adiabatic approximation, is often applied in many FPMD, where the electronic and nuclear motions are solved separately. On the other hand, many phenomena of water on surfaces, such as photo-induced dynamics and electron–phonon couplings, stem from nonadiabatic dynamics, where the electronic evolutions and nuclear motions of the system are strongly coupled. Thus, time-dependent density functional theory (TDDFT) is required, where time-dependent Kohn–Sham equations are numerically solved. With classical nuclear approximations, Ehrenfest dynamics^[28,29] is a practical approach dealing with nonadiabatic excited-state time-domain propagation. Nuclei move in the mean field of electronic potential energy surfaces and forces acting on the nuclei are calculated on-the-fly.

First-principles scheme as we briefly introduced above can be extremely effective at answering the frontier questions, unraveling mechanisms, and providing fundamental insights into the entangled electronic and dynamic properties of water in the proximity of surfaces. In the following, we focus on presenting recent progress in describing the complex interactions and reactions of water with surfaces using first-principles methods. The rest of this review is organized as follows: we discuss water splitting reactions catalyzed by plasmonic metal nanoparticle and metal-free photocatalyst in Sections 2 and 3, respectively. We then focus on the moisture-enhanced corrosion process in Section 4 and address water transport on 2D nanomesh in Section 5. Finally, we give our outlook and conclusions in Section 6.

2. Plasmon-induced water splitting

Plasmonic metal nanostructures combining with oxide semiconductors as a co-catalyst for water splitting have gained increasing attention because of their enormous light harnessing capability and easy tunability of plasmon excitations.^[30–32] One typical example is the titania supported gold nanoparticles (Au/TiO₂ NPs).^[33,34] Upon the excitation wavelength of gold plasmon band, hot electrons with enough energy to overcome the Schottky barrier can be injected from gold NPs to TiO₂, leading to relatively high catalytic performance. On the other hand, the direct injection of hot electrons from plasmonic gold NPs to water molecules, driving water splitting in a Schottky-free junction, was also observed.^[35] High catalytic activity of plasmonic metal clusters is mainly attributed to: (i) field enhancement (FE) induced by elevated electric field near the nanostructure;^[36] and (ii) electron transfer to foreign molecules by nonradiative plasmon decay.^[37]

The golden nanocluster Au₂₀, as shown in Fig. 1, has a large electronic energy gap of 1.77 eV and a unique tetrahedral structure. High surface area provides more adsorption sites for water molecules, indicating possible high activity of photocatalytic water splitting. The ultrafast dynamics and atomic-scale mechanism of water splitting on Au₂₀ cluster stimulated by femtosecond laser pulse were investigated based on *ab initio* real-time time-dependent density functional theory (rt-TDDFT) molecular dynamics.^[31,32] Under the laser pulse with a field strength of 2.3 V/Å and a photon energy of 2.81 eV, corresponding to the dominant peak of the Au₂₀–water adsorption spectrum (see Fig. 1(b)), the dynamic response of water molecules around Au₂₀ cluster is displayed in Fig. 1(c). During the first 10 fs, all O–H bonds in water molecules oscillate near the equilibrium length. Then in response to laser excitation, two water molecules dissociate with O–H bond lengths increasing from around 1 Å to more than 3 Å. Comparison with the case of liquid water without the presence of Au₂₀ cluster, where water molecules remain intact under the same laser irradiation (Fig. 1(d)), confirms that the water splitting is mediated by the Au₂₀ nanocluster. As shown in Fig. 1(e), such process is found to be assisted by rapid proton transport in a Grotthuss-like mechanism,^[38] forming hydronium ions. By analyzing the time-evolved change in the occupation of the Kohn–Sham states, electron transfer from the Au₂₀ cluster to anti-bonding orbital of water is revealed. Furthermore, position-dependent FE for the Au₂₀ cluster shows the same trend as the reaction rate of water splitting, which indicates that the plasmon-induced FE dominantly determines the process, while the commonly assumed electron transfer plays a less important role.^[32]

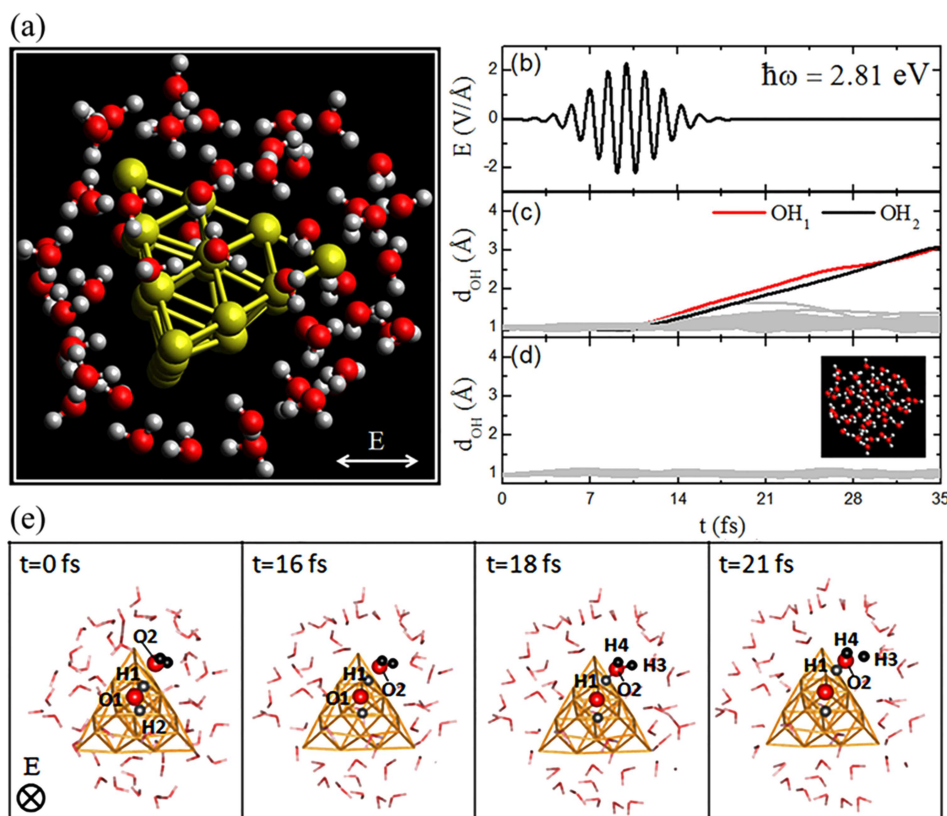


Fig. 1. (a) Snapshot of the Au₂₀ cluster in water, where yellow, red, and grey spheres represent gold, oxygen, and hydrogen atoms, respectively. The arrow denotes polarization direction of the laser field. (b) Time evolution of the laser field with field strength $E_{\max} = 2.3$ V/Å and frequency $\hbar\omega = 2.81$ eV. Under this laser pulse, time-evolved O–H bond lengths d_{OH} of all water molecules with (c) and without (d) Au₂₀ cluster are shown. (e) Atomic configurations at time $t = 0, 16$ fs, 18 fs, and 21 fs. Reprinted with permission from Ref. [32].

3. Water splitting on metal-free photocatalysts

A new perspective on the photocatalytic water splitting is to adopt metal-free carbon photocatalysts, such as modified graphene, carbon nanotubes (CNTs), g-C₃N₄, etc., owing to their nature of non-corrosion, non-toxicity, easy preparation and handling. Many of them show comparable catalytic performances to metal-containing photocatalysts for water splitting. Pristine graphene, known as a zero band-gap semiconductor, in general has no photocatalytic activities. However, its properties can be adjusted by the strategies of heteroatom doping, size modulation, and morphology control, to improve the catalytic activities.^[39] For example, graphite oxide, incorporating oxygen atoms into graphene framework to form sp³ hybridization, opens the bandgap to 2.4–4.3 eV and enables catalyzed hydrogen production under solar irradiation.^[40] Another recent development on ternary boron carbon nitride alloy demonstrated that by doping carbon within hexagonal boron nitride (h-BN) nanosheet, the bandgap of the alloy can be tuned by the amount of incorporated carbon and the hydrogen or oxygen evolution from water can be catalyzed under visible light illumination.^[41]

Among these metal-free photocatalysts, g-C₃N₄ has attracted great attention since it was reported as a potential photocatalyst by Wang and co-workers,^[8] attributed to its high chemical and thermal stability, inexpensiveness, and nontoxic

nature.^[8,42–44] The band gap of g-C₃N₄ is 2.7 eV that is suitable for visible light absorption, and the hydrogen evolution rate can reach 10 μmol/h with the assistance of Pt co-catalyst. As the hydrogen production of g-C₃N₄ is lower than that of metal-containing materials, many efforts have been made to improve the photocatalytic efficiency of g-C₃N₄, such as sulfur doping,^[45,46] single metal atom employing,^[47,48] and carbon dots embedding.^[43] Theoretical calculations based on the DFT have been widely used to study the adsorption configurations^[49–51] and energy profiles of transition states^[52] of water on g-C₃N₄ materials. Although a detailed understanding of the structural and electronic properties of g-C₃N₄ is possible to be gained within the DFT framework, this theory is not viable for revealing the real excitation dynamics of photocatalytic water splitting on g-C₃N₄. For time-dependent processes especially involving excited states, rt-TDDFT and advanced nonadiabatic algorithms are essential.^[53] *Ab initio* rt-TDDFT molecular dynamics investigations of water/g-C₃N₄ interface unveil a three-step mechanism for the photocatalytic water splitting process on g-C₃N₄.^[54] Under photoexcitation, the hole transfer occurs first from carbon to nitrogen atom in g-C₃N₄ sheet, and then a hole current from nitrogen atom to water leads to OH bond weakening in the molecule. Finally, a reverse hole flow from water to nitrogen results in the proton transfer from water to g-C₃N₄. Different from traditional

scheme,^[6,55] the hole transfer plays a key role in the nonadiabatic photocatalytic process and dominates the water splitting stages on $g\text{-C}_3\text{N}_4$.

4. Moisture-enhanced corrosion on plutonium materials

Plutonium is a reactive and radioactive metal. During the handling and storage of the plutonium materials and devices, the metal confronts various environment-dependent chemical corruptions. When exposed to air and moisture, rapid oxidation and corrosion occur on the plutonium metal surface to form a protective layer of plutonium dioxide (PuO_2), which can be further reduced to sesquioxide (Pu_2O_3) by plutonium at the oxide-metal interface. At room temperature, the corrosion rate of plutonium at its equilibrium vapor pressure is hundred times faster than that in dry air. At the boiling point, such moisture enhancement on corrosion rate is increased by five orders of magnitudes.^[56] Understanding the kinetics and mechanism of this moisture-enhanced oxidation process is an important scientific problem in the basic science of actinides and the safe maintenance of nuclear stockpile.

Experimental studies of interactions between water and PuO_2 surface are very challenging. In the early experimental work of Stakebake and co-workers, two distinct temperature ranges of water adsorption on PuO_2 were obtained, suggesting a strong chemisorbed first water layer and a weak physisorbed second layer, with estimated adsorption energies of -2.94 eV and -0.88 eV, respectively.^[57] Paffet *et al.* supported the microscopic structure of water/ PuO_2 interface depicted above and further revised the adsorption energies to -1.82 eV and -1.11 eV for the dissociative and molecular adsorptions, respectively.^[58] Most theoretical studies on the water interactions with the PuO_2 surfaces have focused on the adsorption geometries and energies.^[59–62] Recently, the dynamics and mechanism of water dissociation on the PuO_2 surface have been reported.^[63] Using FPMD simulations with the DFT+ U approach, a two-step hydroxylation process for water dissociation on the PuO_2 (110) surface is observed. Despite the same dissociation steps, the reaction mechanisms are different for water single molecule and small clusters. As the results of hybridizations between the molecular orbitals of water and the electronic state of the top surface, water monomer dissociation requires an activation energy of 0.18 eV, in contrast to the case of water dimer where the dissociation is an exothermic reaction with no energy barrier. Such promotion in the water cluster dissociation can be attributed to the hydrogen-bonding interactions between water molecules, which initiate the process from the hydrogen bond acceptor molecule, yielding a more stable dissociation state with respect to a single molecule, as illustrated in Fig. 2. The effect of surface vacancy on the water dissociation process was discussed in Ref. [64].

A major dissociation preference of water molecule for the oxygen vacancy site on the PuO_2 surface is found and it is independent of water or vacancy coverage.

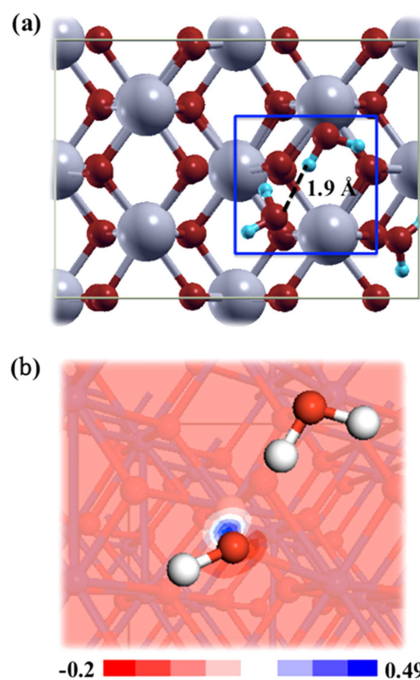


Fig. 2. (a) Configuration of the initiation step of water trimer dissociation on the PuO_2 (110) surface. (b) Electron density difference contour of the configuration shown in (a). Reprinted with permission from Ref. [63].

Plutonium sesquioxide, formed at the plutonium oxide-metal interface, also plays an important role in the water enhanced corrosion process of plutonium material. Two phases exist with different crystalline structures for Pu_2O_3 : cubic ($\alpha\text{-Pu}_2\text{O}_3$) and hexagonal ($\beta\text{-Pu}_2\text{O}_3$) crystals. The former is stable below ~ 350 K while the latter is only stable at high temperatures.^[65,66] The $\alpha\text{-Pu}_2\text{O}_3$ can be obtained by removing 25 percent of oxygen atoms from eight fluorite PuO_2 unit cells. Adsorption, diffusion, and dissociation behaviors of water molecule on the $\alpha\text{-Pu}_2\text{O}_3$ (111) surface have been studied by combining FPMD and nudged elastic band (NEB) methods.^[67] It is shown that with very low absorption energy and diffusion barrier, water molecule tends to diffuse more than dissociate on the surface at low temperature. In FPMD simulations, the decomposition of water molecule into H and OH is only observed at 900 K.

5. Water purification with graphdiyne membrane

Water purification and desalination are of great importance to industry and agriculture in modern society.^[11–13] Membrane technology is widely used in water desalination and ion separation.^[68] Recently, two-dimensional materials, e.g., graphene, graphene oxides, and h-BN, have been shown to have good molecular permeability and selectivity.^[10,69,70] The molecular conductivity originates from the nanoscale

transport channels, including the nanopores on membrane planes^[71,72] and the nanochannel between adjacent layers.^[1,73,74] The conductivity of various species can be adjusted by precisely controlling the size of the transport channel, so as to improve the molecular selectivity. Despite of the intrinsic trade-off, the ultimate goal of membrane technology is to achieve both high molecular conductivity and selectivity.

Two-dimensional nanomesh materials have large nanopore density and perfect uniformity, and thus are considered as excellent candidate materials for molecular sieving. Graphdiyne,^[75] a novel two-dimensional carbon allotrope, as shown in Fig. 3(a), has attracted great attention because of its exceptional mechanical, physical, and chemical properties.^[76–79] Early classical molecular dynamics (CMD) simulations showed that graphdiyne is impermeability for water molecule,^[80,81] while first-principles calculations instead pointed out the possibility of water conductivity when considering the transmembrane interaction.^[82] More recently, water

transportability of graphdiyne has been studied by extensive FPMD and *ab-initio* parameterized CMD simulations.^[83] It is revealed that water molecules can permeate through graphdiyne membrane with a relatively large flow rate at high external pressure, as shown in Fig. 3(b). The flow rate can be written as $\Phi = A_0 \exp(-E_a/(k_B T))$. The activation energy E_a can be estimated as $E_a = E_{\text{mem}} + E_{\text{water}} - PV$, where E_{mem} and E_{water} are the contributions from the membrane and other water molecules through hydrogen bonding, respectively, and PV represents the effect of pressure and temperature. The activation energy can be directly modulated by pressure, leading to a nonlinear dependence of water flow on pressure. Therefore, the activated water flow in graphdiyne can be precisely controlled by adjusting the working pressure. Further analysis of the atomistic dynamics of water molecules shows that a transmembrane hydrogen bond is formed and a unique two-hydrogen-bond structure acts as transient state in the process of water transport.^[83]

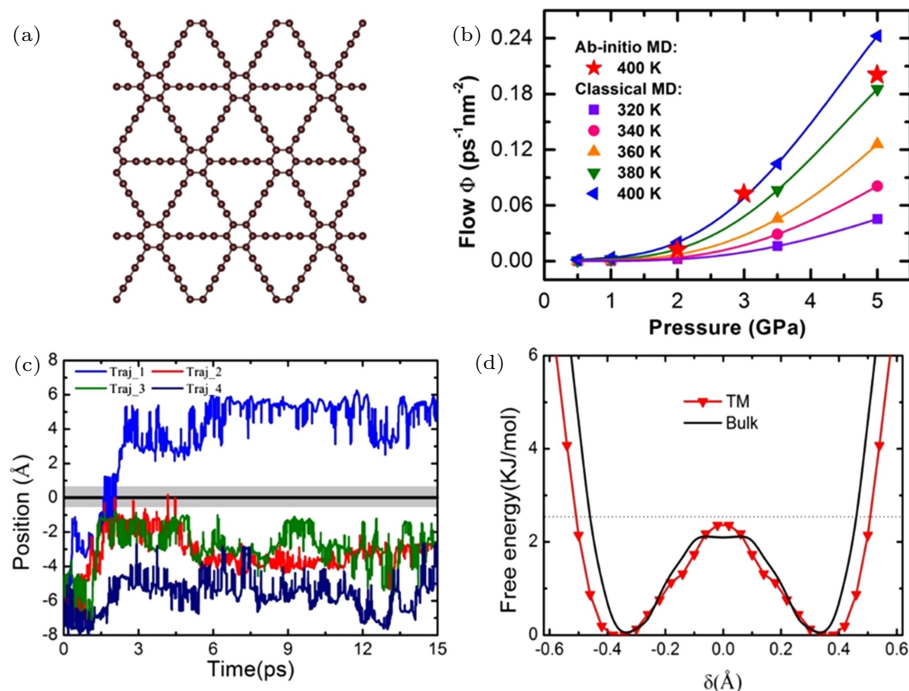


Fig. 3. (a) The atomistic structure of graphdiyne. (b) The water flow across graphdiyne versus temperature and pressure. (c) the trajectories of proton diffusion at the water-graphdiyne interface. (d) The free energy barrier for transmembrane (TM) proton transfer and proton transfer in bulk water. The dash line indicates the $k_B T$ at 300 K. Reprinted with permission from Ref. [84].

Considering the Grotthuss mechanism of proton hopping, the transmembrane hydrogen bond could be an efficient bridge for transmembrane proton transport. As shown in Fig. 3(c), a proton diffuses across graphdiyne membrane in Traj_1 under unbiased conditions, indicating that the thermal fluctuations are the driven force for transmembrane proton transport.^[84] Free energy calculations for proton transfer display the energy barrier of transmembrane proton transfer is nearly the same as that of bulk water, and both energy barriers are smaller than $k_B T$. Proton conductivity of graphdiyne, obtained with FPMD simulations under electric field, is $0.6 \text{ S}\cdot\text{cm}^{-1}$, one or-

der of magnitude larger than that of Nafion.^[85] The appropriate nanopore size of graphdiyne can hinder the transport of ions and soluble fuel molecules, and give graphdiyne superior proton selectivity. Therefore, graphdiyne as a proton exchange membrane in fuel cell has a promising application prospect.

6. Outlook and conclusions

In summary, we discussed recent progress on understanding the complex interplay between the electronic and structural properties of water interacting with surfaces, using first-

principles techniques. This is presented as an example of novel phenomena emerging when assembling different levels of theoretical blocks to investigate the physiochemical properties of water at nanoscale. The future challenge will be to achieve integration of advanced computational approaches and to define general validation strategies appropriate for broad classes of water systems.

At present, the first-principles dynamic simulations of water commonly ignore part of the quantum effect of particles, especially the quantum effect of nuclei and non-adiabatic dynamic effect. As the lightest element, the nuclear quantum effect of hydrogen is especially prominent in the structure and dynamics of water. To develop a set of numerical simulation methods for the total quantization of hydrogen and to quantize the electron and nucleus at the same time will break through the bottleneck of current computational simulation research and provide a new framework to accurately describe the hydrogen bond structure, interactions between water and different materials, and dynamic mechanisms of transport and reactions.

References

- [1] Chen L, Shi G, Shen J, Peng B, Zhang B, Wang Y, Bian F, Wang J, Li D, Qian Z, Xu G, Liu G, Zeng J, Zhang L, Yang Y, Zhou G, Wu M, Jin W, Li J and Fang H 2017 *Nature* **550** 380
- [2] Shi G, Chen L, Yang Y, Li D, Qian Z, Liang S, Yan L, Li L H, Wu M and Fang H 2018 *Nat. Chem.* **10** 776
- [3] Velasco-Velez J J, Wu C H, Pascal T A, Wan L F, Guo J, Prendergast D and Salmeron M 2014 *Science* **346** 831
- [4] Guo J, Lü J T, Feng Y, Chen J, Peng J, Lin Z, Meng X, Wang Z, Li X Z, Wang E G and Jiang Y 2016 *Science* **352** 321
- [5] Zou X and Zhang Y 2015 *Chem. Soc. Rev.* **44** 5148
- [6] Kudo A and Miseki Y 2009 *Chem. Soc. Rev.* **38** 253
- [7] Maeda K and Domen K 2007 *J. Phys. Chem. C* **111** 7851
- [8] Wang X, Maeda K, Thomas A, Takanabe K, Xin G, Carlsson J M, Domen K and Antonietti M 2009 *Nat. Mater.* **8** 76
- [9] Wang Y, Suzuki H, Xie J, Tomita O, Martin D J, Higashi M, Kong D, Abe R and Tang J 2018 *Chem. Rev.* **118** 5201
- [10] Buelke C, Alshami A, Casler J, Lewis J, Al-Sayaghi M and Hickner M A 2018 *Desalination* **448** 113
- [11] Pendergast M M and Hoek E M V 2011 *Energy Environ. Sci.* **4** 1946
- [12] Shannon M A, Bohn P W, Elimelech M, Georgiadis J G, Marinas B J and Mayes A M 2008 *Nature* **452** 301
- [13] Elimelech M and Phillip W A 2011 *Science* **333** 712
- [14] Hohenberg P and Kohn W 1964 *Phys. Rev.* **136** B864
- [15] Kohn W and Sham L J 1965 *Phys. Rev.* **140** A1133
- [16] Perdew J P, Burke K and Ernzerhof M 1996 *Phys. Rev. Lett.* **77** 3865
- [17] Schwegler E, Grossman J C, Gygi F and Galli G 2004 *J. Chem. Phys.* **121** 5400
- [18] Grossman J C, Schwegler E, Draeger E W, Gygi F and Galli G 2004 *J. Chem. Phys.* **120** 300
- [19] Burke K 2012 *J. Chem. Phys.* **136** 150901
- [20] Zhang C, Donadio D, Gygi F and Galli G 2011 *J. Chem. Theory Comput.* **7** 1443
- [21] Wang J, Roman-Perez G, Soler J M, Artacho E and Fernandez-Serra M V 2011 *J. Chem. Phys.* **134** 024516
- [22] Ataca C, Sahin H and Ciraci S 2012 *J. Phys. Chem. C* **116** 8983
- [23] Singh A K, Mathew K, Zhuang H L and Hennig R G 2015 *J. Phys. Chem. Lett.* **6** 1087
- [24] Sun J, Ruzsinszky A and Perdew J P 2015 *Phys. Rev. Lett.* **115** 036402
- [25] Sun J, Remsing R C, Zhang Y, Sun Z, Ruzsinszky A, Peng H, Yang Z, Paul A, Waghmare U, Wu X, Klein M L and Perdew J P 2016 *Nat. Chem.* **8** 831
- [26] Liechtenstein A I, Anisimov V V and Zaanen J 1995 *Phys. Rev. B* **52** R5467
- [27] Dudarev S L, Botton G A, Savrasov S Y, Humphreys C J and Sutton A P 1998 *Phys. Rev. B* **57** 1505
- [28] C. Tully J 1998 *Faraday Discuss.* **110** 407
- [29] Meng S and Kaxiras E 2008 *J. Chem. Phys.* **129** 054110
- [30] Linic S, Christopher P and Ingram D B 2011 *Nat. Mater.* **10** 911
- [31] Yan L and Meng S 2017 *Sci. China-Phys. Mech. Astron.* **60** 027032
- [32] Yan L, Xu J, Wang F and Meng S 2018 *J. Phys. Chem. Lett.* **9** 63
- [33] Gomes Silva C, Juárez R, Marino T, Molinari R and García H 2011 *J. Am. Chem. Soc.* **133** 595
- [34] Awate S V, Deshpande S S, Rakesh K, Dhanasekaran P and Gupta N M 2011 *Phys. Chem. Chem. Phys.* **13** 11329
- [35] Robatjazi H, Bahaeddin S M, Doiron C and Thomann I 2015 *Nano Lett.* **15** 6155
- [36] Kang J H, Kim D S and Park Q H 2009 *Phys. Rev. Lett.* **102** 093906
- [37] Yan L, Wang F and Meng S 2016 *ACS Nano* **10** 5452
- [38] Rini M, Magnes B Z, Pines E and Nibbering E T J 2003 *Science* **301** 349
- [39] Xu Y, Kraft M and Xu R 2016 *Chem. Soc. Rev.* **45** 3039
- [40] Yeh T F, Syu J M, Cheng C, Chang T H and Teng H 2010 *Adv. Funct. Mater.* **20** 2255
- [41] Huang C, Chen C, Zhang M, Lin L, Ye X, Lin S, Antonietti M and Wang X 2015 *Nat. Commun.* **6** 7698
- [42] Dai L, Xue Y, Qu L, Choi H J and Baek J B 2015 *Chem. Rev.* **115** 4823
- [43] Liu J, Liu Y, Liu N, Han Y, Zhang X, Huang H, Lifshitz Y, Lee S T, Zhong J and Kang Z 2015 *Science* **347** 970
- [44] Jiao Y, Zheng Y, Chen P, Jaroniec M and Qiao S Z 2017 *J. Am. Chem. Soc.* **139** 18093
- [45] Liu G, Niu P, Sun C, Smith S C, Chen Z, Lu G Q and Cheng H M 2010 *J. Am. Chem. Soc.* **132** 11642
- [46] Zhang J, Sun J, Maeda K, Domen K, Liu P, Antonietti M, Fu X and Wang X 2011 *Energy Environ. Sci.* **4** 675
- [47] Li X, Bi W, Zhang L, Tao S, Chu W, Zhang Q, Luo Y, Wu C and Xie Y 2016 *Adv. Mater.* **28** 2427
- [48] Zhang L, Long R, Zhang Y, Duan D, Xiong Y, Zhang Y and Bi Y 2020 *Angew. Chem. Int. Ed.* **59** 6224
- [49] Wu H Z, Liu L M and Zhao S J 2014 *Phys. Chem. Chem. Phys.* **16** 3299
- [50] Aspera S M, David M and Kasai H 2010 *Jpn. J. Appl. Phys.* **49** 115703
- [51] Wu H Z, Liu L M and Zhao S J 2015 *Appl. Surf. Sci.* **358** 363
- [52] Steinmann S N, Melissen S T A G, Le Bahers T and Sautet P 2017 *J. Mater. Chem. A* **5** 5115
- [53] You P W, Chen D Q, Lian C, Zhang C and Meng S 2020 *WIREs Comput. Mol. Sci.* e1492
- [54] You P W, Lian C, Xu J Y, Zhang C and Meng S 2020 submitted
- [55] Ma H, Feng J, Jin F, Wei M, Liu C and Ma Y 2018 *Nanoscale* **10** 15624
- [56] Haschke J M, Allen T H and Martz J C 1998 *J. Alloys Compd.* **271–273** 211
- [57] Stakebake J L 1973 *The Journal of Physical Chemistry* **77** 581
- [58] Paffett M T, Kelly D, Joyce S A, Morris J and Veirs K 2003 *J. Nucl. Mater.* **322** 45
- [59] Wu X and Ray A K 2002 *Phys. Rev. B* **65** 085403
- [60] Jomard G, Bottin F and Geneste G 2014 *J. Nucl. Mater.* **451** 28
- [61] Tegner B E, Molinari M, Kerridge A, Parker S C and Kaltsoyannis N 2017 *J. Phys. Chem. C* **121** 1675
- [62] Wellington J P W, Kerridge A, Austin J and Kaltsoyannis N 2016 *J. Nucl. Mater.* **482** 124
- [63] Zhang C, Yang Y and Zhang P 2017 *J. Phys. Chem. C* **122** 371
- [64] Zhang C, Yang Y and Zhang P 2019 *Sci. China-Phys. Mech. Astron.* **62** 107002
- [65] Petit L, Svane A, Szotek Z, Temmerman W M and Stocks G M 2010 *Phys. Rev. B* **81** 045108
- [66] Keller C 1973 *Comprehensive Inorganic Chemistry*, Bailar J C, et al. eds. (Oxford: Pergamon) pp. 219–276
- [67] Wang X X, Wang S, Zhang C, Yang Y and Zhang P 2019 *J. Phys.: Condens. Matter* **31** 265001
- [68] Cheng Y, Ying Y, Japip S, Jiang S D, Chung T S, Zhang S and Zhao D 2018 *Adv. Mater.* **30** 1870355

- [69] Prozorovska L and Kidambi P R 2018 *Adv. Mater.* **30** e1801179
- [70] Wang L, Boutilier M S H, Kidambi P R, Jang D, Hadjiconstantinou N G and Karnik R 2017 *Nat. Nanotechnol.* **12** 509
- [71] Achtyl J L, Unocic R R, Xu L, Cai Y, Raju M, Zhang W, Sacchi R L, Vlassiuk I V, Fulvio P F, Ganesh P, Wesolowski D J, Dai S, van Duin A C, Neurock M and Geiger F M 2015 *Nat. Commun.* **6** 6539
- [72] Surwade S P, Smirnov S N, Vlassiuk I V, Unocic R R, Veith G M, Dai S and Mahurin S M 2015 *Nat. Nanotechnol.* **10** 459
- [73] Nair R R, Wu H A, Jayaram P N, Grigorieva I V and Geim A K 2012 *Science* **335** 442
- [74] Joshi R K, Carbone P, Wang F C, Kravets V G, Su Y, Grigorieva I V, Wu H A, Geim A K and Nair R R 2014 *Science* **343** 752
- [75] Li G, Li Y, Liu H, Guo Y, Li Y and Zhu D 2010 *Chem. Commun.* **46** 3256
- [76] Jia Z, Li Y, Zuo Z, Liu H, Huang C and Li Y 2017 *Acc. Chem. Res.* **50** 2470
- [77] Gao X, Liu H, Wang D and Zhang J 2019 *Chem. Soc. Rev.* **48** 908
- [78] Huang C, Li Y, Wang N, Xue Y, Zuo Z, Liu H and Li Y 2018 *Chem. Rev.* **118** 7744
- [79] Li Y, Xu L, Liu H and Li Y 2014 *Chem. Soc. Rev.* **43** 2572
- [80] Xue M, Qiu H and Guo W 2013 *Nanotechnology* **24** 505720
- [81] Zhu C, Li H, Zeng X C, Wang E G and Meng S 2013 *Sci. Rep.* **3** 3163
- [82] Bartolomei M, Carmona-Novillo E, Hernandez M I, Campos-Martinez J, Pirani F, Giorgi G and Yamashita K 2014 *J. Phys. Chem. Lett.* **5** 751
- [83] Xu J, Zhu C, Wang Y, Li H, Huang Y, Shen Y, Francisco J S, Zeng X C and Meng S 2018 *Nano Res.* **12** 587
- [84] Xu J, Jiang H, Shen Y, Li X Z, Wang E G and Meng S 2019 *Nat. Commun.* **10** 3971
- [85] Ochi S, Kamishima O, Mizusaki J and Kawamura J 2009 *Solid State Ionics* **180** 580